Available online at www.sciencedirect.com
ScienceDirect
Developmental Biology 305 (2007) 599–614
DEVELOPMENTAL BIOLOGY
www.elsevier.com/locate/ydbio

Paracrine and autocrine mechanisms of apelin signaling govern embryonic and tumor angiogenesis

Roland E. Kälin [a], Martin P. Kretz [a], Andrea M. Meyer [a], Andreas Kispert [b], Frank L. Heppner [c], André W. Brändli [a,*]

[a] Institute of Pharmaceutical Sciences, Department of Chemistry and Applied Biosciences, ETH Zurich, Wolfgang-Pauli-Strasse 10, CH-8093 Zurich, Switzerland
[b] Institute of Molecular Biology, Hannover Medical School, Hannover, Germany
[c] Institute of Neuropathology, University Hospital Zurich, Zurich, Switzerland

Received for publication 8 November 2006; revised 2 March 2007; accepted 6 March 2007
Available online 12 March 2007

Abstract

Apelin and its G protein-coupled receptor APJ play important roles in blood pressure regulation, body fluid homeostasis, and possibly the modulation of immune responses. Here, we report that apelin-APJ signaling is essential for embryonic angiogenesis and upregulated during tumor angiogenesis. A detailed expression analysis demonstrates that both paracrine and autocrine mechanisms mark areas of embryonic and tumor angiogenesis. Knockdown studies in *Xenopus* reveal that apelin-APJ signaling is required for intersomitic vessel angiogenesis. Moreover, ectopic expression of apelin but not vascular endothelial growth factor A (VEGFA) is sufficient to trigger premature angiogenesis. *In vitro*, apelin is non-mitogenic for primary human endothelial cells but promotes chemotaxis. Epistasis studies in *Xenopus* embryos suggest that apelin-APJ signaling functions downstream of VEGFA. Finally, we show that apelin and APJ expression is highly upregulated in microvascular proliferations of brain tumors such as malignant gliomas. Thus, our results define apelin and APJ as genes of potential diagnostic value and promising targets for the development of a new generation of anti-tumor angiogenic drugs.

Keywords: Angiogenesis; Apelin; APJ; Cancer; Glioblastoma; Mouse; Signal transduction; VEGF; Xenopus

Introduction

Glioblastoma multiforme (GBM) is the most malignant glioma with an invasive and destructive growth pattern. It presents with increased mitotic activity, tumor necrosis, and pronounced angiogenesis (Kleihues et al., 2002). Clinically, patients diagnosed with GBM show a median survival of less than a year despite aggressive surgery, radiation, and chemotherapy (Holland, 2001). Current anti-GBM treatment modalities including radiotherapy plus concomitant and adjuvant temozolomide (Stupp et al., 2005) provide a modest survival advantage at best and, hence, alternative therapeutic approaches are urgently needed.

Tumor angiogenesis is one of the pathological hallmarks of malignant gliomas (Plate and Risau, 1995), which, in turn, makes the control of tumor blood supply a promising therapeutic target. Vascular endothelial growth factors, particularly VEGFA, are considered to be the most important proangiogenic factors in pathologic angiogenesis (Ferrara et al., 2003). VEGFA is overexpressed in most GBMs, and its receptors are present at high levels on the tumor vessels (Hatva et al., 1995; Plate et al., 1992). Furthermore, studies using orthotopic animal models indicate that glioma growth and vascularization is strongly VEGFA dependent and, vice versa, inhibition of VEGFA signaling significantly halts glioma growth by blocking neovascularization and proliferation (Goldbrunner et al., 2000; Goldbrunner et al., 2004).

Given the importance of VEGFA in tumor angiogenesis, much attention has focused on developing anti-VEGF or anti-VEGF receptor (VEGFR) therapies to treat a variety of cancers. In the last years, various clinical trials have demonstrated the efficiency of anti-VEGF therapies (Kerbel, 2006). More recently, however, drug resistance by evasion of VEGF inhibition

* Corresponding author. Fax: +41 44 633 1358.
E-mail address: brandli@pharma.ethz.ch (A.W. Brändli).

0012-1606/$ - see front matter © 2007 Elsevier Inc. All rights reserved.
doi:10.1016/j.ydbio.2007.03.004

through upregulation of additional angiogenic factors has been reported to occur in preclinical settings (Casanovas et al., 2005; Mizukami et al., 2005). Hence, the identification and development of alternative drug targets to prolong the effectiveness of antiangiogenic drugs is pertinent.

APJ (putative receptor protein related to the angiotensin receptor AT1; angiotensin II related receptor-like 1—Agtrl1) and its amphibian orthologue Msr encode members of the G protein-coupled receptor (GPCR) gene family that have been implicated in the control of blood vessel development (Devic et al., 1996; Devic et al., 1999). Originally identified as orphan GPCRs, APJ and Msr are structurally related to the angiotensin II receptor type I (AT1R) (Devic et al., 1996; O'Dowd et al., 1993) but despite the significant structural homology, angiotensin II does not bind to APJ (Tatemoto et al., 1998). Apelin, the natural ligand of APJ was isolated from bovine stomach (Tatemoto et al., 1998). In mammals, the apelin gene encodes a secreted preprotein of 77 amino acids with a signal peptide, a prodomain, and a C-terminal peptide, which upon proteolytic maturation generates a number of apelin polypeptides (Tatemoto et al., 1998). Apelin-36, comprised of amino acids 42–77, and apelin-13 (amino acids 65–77) represent the predominant and most active isoforms (Hosoya et al., 2000; Tatemoto et al., 1998). In the adult, apelin and its receptor are expressed both in the brain and in the periphery, particularly in the gastrointestinal tract, adipose tissues, lung, kidney, liver, and the skeletal muscle. In addition, APJ and apelin are highly expressed in the cardiovascular system, where they play important physiological roles in the regulation of blood pressure and cardiac contractility (Kleinz and Davenport, 2005; Masri et al., 2005). During postnatal development, apelin signaling is also associated with retinal blood vessels, where it may function to regulate angiogenesis (Kasai et al., 2004; Saint-Geniez et al., 2002). The role of apelin-APJ signaling in embryonic angiogenesis and its significance for pathologic angiogenesis has, however, remained largely elusive. While this manuscript was in preparation, two studies reporting contradicting results about the role of apelin signaling during cardiovascular development in the *Xenopus* embryo were published (Cox et al., 2006; Inui et al., 2006). Cox et al. demonstrate that apelin and APJ play important roles in blood vessel morphogenesis, where they are required for the formation of intersomitic vessels. In contrast, the study of Inui et al. suggests that apelin and APJ play more general roles in cardiovascular development by regulating differentiation of endothelia, hematopoietic cells, and cardiomyocytes.

Here we provide novel mechanistic insights into the role of apelin-APJ signaling during blood vessel formation under normal and pathological conditions. Apelin expression is associated with angiogenic blood vessel growth, where it acts via paracrine and autocrine mechanisms. We demonstrate that apelin-APJ signaling is necessary and sufficient to promote angiogenic blood vessel growth *in vivo*. Interestingly, we failed to observe in our loss-of-function studies any evidence of general defects in cardiovascular development supporting the view of a primary role of apelin signaling in angiogenesis. Epistasis analysis in *Xenopus* embryos suggests that apelin signaling functions downstream of VEGFA. Finally, we provide evidence for an important role of apelin and APJ in tumor angiogenesis, namely to pathological vessel formation in GBM. Taken together, our studies identify apelin and its receptor APJ as novel targets for anti-angiogenic tumor therapies.

Materials and methods

Cloning of cDNAs, sequencing, and sequence analysis

Expressed sequence tag (EST) databases were screened for potential *Xenopus laevis* cDNAs related to human apelin, APJ and VEGFA. For each gene, multiple cDNAs were identified and retrieved. Sequence comparisons revealed that each human gene was represented by two classes of cDNAs, which are likely to be derived from two pseudoallelic gene variants present in the *X. laevis* genome. *Xenopus* cDNAs for apelin-a (GenBank Acc. No. BE680255), APJa (AW460831), APJb (BQ399449, BQ724849, BQ726502), VEGFAb (BF426570) were obtained from the RZPD German Resource Center for Genome Research. *Xenopus* cDNAs for apelin-b (BJ030743) and APJb (BJ033869) were kindly provided by the NIBB *X. laevis* EST Project, Japan. Double-stranded DNA sequencing was either performed in-house or by Primm srl, Italy. Assembly of nucleotide sequence traces, analysis of nucleotide and protein sequences was performed using the DNAStar Lasergene software package (version 6.0). Amino acid sequence alignments were performed with MegAlign (DNAStar) using the Clustal W algorithm and the PAM250 residue weight table. The alignments then were used to construct phylogenetic trees with the Neighbor-Joining algorithm (Saitou and Nei, 1987). The described *Xenopus* nucleotide sequences were deposited with GenBank: apelin-a (GenBank Acc. No. DQ471852), apelin-b (DQ471853), APJa (DQ473441), APJb (DQ473442), and VEGFAb168 (DQ481238).

Plasmid constructs

The following constructs were generated for *in vitro* coupled transcription–translation reactions and/or *in vitro* RNA synthesis. Plasmid Apelin-ORF contains the ORF of *Xenopus* apelin-a (Gene Bank Acc. No. DQ471852). Plasmid Apelin-(5′)-UTR encodes 18 nucleotides of the 5′UTR followed by the ORF of apelin-a. Plasmid Apelin (F13A) contains the complete ORF of apelin-a but the carboxy-terminal phenylalanine was substituted by alanine. Plasmid APJa-ORF contains the ORF plus 118 nucleotides of the 3′UTR of *Xenopus* APJa (DQ473441). Plasmid APJa-(5′)-UTR contains 36 nucleotides of the 5′UTR and the ORF of APJa. Plasmid APJb-ORF contains 43 nucleotides of the 5′UTR, the ORF, and 89 nucleotides of the 3′UTR of *Xenopus* APJb (DQ473442). Plasmid VEGFA-ORF contains the ORF of *Xenopus* VEGFAb (isoform 4, VEGFA168, DQ481238). Plasmid VEGFA-MIS contains essentially the ORF of *Xenopus* VEGFAb (DQ481238), but seven point mutations were introduced which encode the original amino acid sequence but no longer serve as a target for the VEGFA-MO (see below). All plasmids were generated by PCR using the Expand High Fidelity PCR System (Roche Diagnostics) and subcloned into the pCS2+ vector (Turner and Weintraub, 1994). The constructs were confirmed by DNA sequencing.

Xenopus embryo manipulations, in situ hybridization, and sectioning

In vitro fertilization, culture and staging of *Xenopus* embryo were performed as described (Brändli and Kirschner, 1995; Helbling et al., 1998). Probe synthesis, whole mount *in situ* hybridization, β-galactosidase staining, and bleaching of *Xenopus* embryos were carried out as described (Helbling et al., 1999; Helbling et al., 1998; Saulnier et al., 2002). In some cases, embryos were immersed into clearing solution (2:1 benzyl benzoate/benzyl alcohol) to visualize staining of internal structures. Digoxigenin-labeled probes were synthesized from linearized plasmids encoding *Xenopus* Msr (Devic et al., 1996), APJb (GenBank Acc. No. DQ473442), apelin-a (DQ471852), Erg (Baltzinger et al., 1999), Fli1 (Meyer et al., 1995), VEGFR2 (BJ075253), VEGFR1 (BQ736 324), Gata3 (Bertwistle et al., 1996), αT3-globin (Banville and Williams, 1985), Pecam1 (BF612503), and Tie2 (Iraha et al., 2002). Sense strand controls were prepared from all plasmids and tested negative by *in situ* hybridization.

Fixed *Xenopus* embryos stained in whole mount were embedded in 4% low-melt agarose for sectioning with a vibrating blade microtome (Leica VT1000S) as described previously (Eid and Brändli, 2001). Pictures were taken using either bright-field or Normarski optics.

Microinjection of Xenopus embryos

The following morpholino oligonucleotides (MO) were ordered from Gene Tools LLC (Corvallis, OR) to inhibit translation of *Xenopus* mRNAs (initiation codons are underlined; mispaired nucleotides are indicated with small letters): Apelin-MO, 5′-GTCTGAGATTCATGTTTCTTGTGGC-3′ (which targets apelin-a and apelin-b); Apelin-MO(mp), 5′-GTCTGtGATTgATGTaTCTTcTGGC-3′; APJ-MO, 5′-CTGTGTGGAAGCAATAGAAAGTCCT-3′ (which targets the 5′UTR of APJ-a and APJ-b); APJ-MO(mp), 5′-TGaGTGcAAGCtATAGAAtGTCCT-3′, VEGFA-MO, 5′-GATCCAGCTCGGCAGAAAGTTCATG-3′ (which targets both VEGFAa and VEGFAb); VEGFA-MO(mp), 5′-GATgCAGgTCcGCAcAAAGTTgATG-3′. *In vitro* coupled transcription–translation reactions and MO injections were performed as described (Saulnier et al., 2002). If not indicated differently, 0.1 to 10 ng of each MO were injected per single blastomeres of two-cell-stage embryos. RNA synthesis and microinjections were performed as described (Helbling et al., 1998) except that purification was done by phenol–chloroform extraction. For rescue experiments, mRNA was synthesized using plasmid Apelin-ORF as a template. In some experiments, mRNA injections were performed into V2 or D2 blastomeres of 8-cell stage embryos (Moody and Kline, 1990). RNA encoding the lineage tracer nuclear β-galactosidase (nucβgal) was usually coinjected at 0.25 ng per blastomere.

Whole mount in situ hybridization of mouse embryos

Mouse embryos were obtained from matings of NMRI wildtype animals. For timed pregnancies plugs were checked in the morning after mating, noon was taken as 0.5 days post coitum (d.p.c.). Embryos were fixed in 4% PFA and stored in 100% methanol at −20 °C prior to *in situ* hybridization analysis. Whole-mount *in situ* hybridization on mouse embryos was essentially performed following a standard procedure (Wilkinson, 1992). Digoxigenin-labeled probes were transcribed from linearized plasmids encoding mouse APJ (GenBank Acc. No. AA098426) and apelin (BG176301). Stained specimens were transferred into 80% glycerol for documentation.

Establishment of CHO cells stably expressing Xenopus APJ-EGFP

Flp-In-CHO-K1 cells (R75807; Invitrogen) were used to create a cell line stably expressing the *Xenopus* APJ-EGFP fusion protein under the control of the human cytomegalovirus immediate-early enhancer/promotor. The full open reading frame (ORF) of *X. laevis* Msr/APJa (Devic et al., 1996) was amplified by PCR and subcloned in-frame into the *Xho*I and *Hin*dIII sites of pEGFP-N1 vector (#U55762; BD Biosciences). The resulting plasmid was digested with *Nhe*I and *Not*I and the APJ-EGFP cDNA was subcloned into pcDNA5/FRT vector (Invitrogen) to generate the Flp-In expression vector pcDNA5/FRT/APJ-EGFP. Cotransfections of pcDNA5/FRT/APJ-EGFP and pOG44 into Flip-In-CHO-K1 cells were done using the FuGENE6 transfection reagent (Roche) and selections were performed according to the manufacturer's instructions. Transfected cells were evaluated by fluorescence microscopy for APJ-EGFP expression at the cell surface. The resulting Flp-In-CHO-APJ-EGFP (in short: CHO-APJ) cell line was grown at 37 °C in DMEM growth medium (DMEM containing 10% FCS and 1% penicillin–streptomycin solution; GIBCO/Invitrogen) under standard techniques.

Internalization assays

CHO-APJ cells were diluted in DMEM growth medium and seeded (200 µl/well) on 8-well glass slides (Lab-Tek Chamber Slides, Nunc). The cells were cultured overnight at 37 °C to 70–90% confluency. Apelin-13 (pyroglutamylated apelin-13; # H-4568, Bachem) and angiotensin II (#H-1705, Bachem) were dissolved at different concentrations (0.1, 0.2, 0.5 and 1 µM) in DMEM containing 1% BSA. To initiate the assay, the cells were washed with 0.5 ml PBS and treated with apelin-13 or angiotensin II peptides in DMEM/1% BSA for 0, 30, 60 or 120 min at 37 °C. Cells were washed with PBS at 4 °C and fixed in fixation buffer (4% paraformaldehyde in PBS) for 15 min. Cells were washed with 0.1 M glycine in PBS, and then with PBS. To stain nuclei, cells were incubated with 3 µg/ml DAPI in PBS for 1 min and washed with PBS. Samples were mounted in Citifluor AF-1 mounting medium (Citifluor Ltd.). Cells were examined under a fluorescent microscope (Axioskop, Zeiss) and pictures were taken using a confocal laser scanning microscope (CLSM 410, Zeiss). Picture stacks were processed on a silicon graphics workstation using Imaris software (Bitplane).

cAMP assays

CHO-APJ cells were seeded into black 96-well plates (Costar) at a density of 65,000 cells/cm^2 and grown for 1 day. The growth medium was replaced by PBS containing 0.2 mM 3-isobutyl-1-methylxanthine (IBMX, Sigma) to initiate the assay. After 45 min, an equal volume of PBS containing 0.2 mM IBMX, 2 µM forskolin (Sigma) and apelin-13 (final concentration ranging from 0 to 8 µM) was added. After 30 min at 37 °C, the cAMP levels were measured with the cAMP Fluorescence Polarization Biotrak Immunoassay System (Amersham) using a fluorescence plate reader (GENios Pro, Tecan). The fluorescence polarization was measured according to the manufacturer's recommendation. CHO-APJ treated with forskolin alone served as reference. The parental Flip-In-CHO-K1 cells, which do not express APJ, were used as a background control. The inhibition of cAMP production was calculated as mean ± standard deviation of triplicate assays.

Human endothelial cell culture

Culture media and primary human endothelial cells (umbilical vein endothelial cells, HUVEC, #CC-2519; umbilical arterial endothelial cells, HUAEC, #CC-2520; dermal microvascular endothelial cells, HMVEC-D, #CC-2516) were obtained from Cambrex. Endothelial cells were cultured either in EGM-2 (for HUVEC) or EGM-2-MV (HUAEC, HMVEC-D) according to the supplier's recommendations. The cells were used up to passage 5.

RT-PCR assays

For standard RT-PCR, total RNA was extracted from HUVEC and HUAEC cultures (90% confluency) with TRIzol reagent (Invitrogen) according to the manufacturer's instructions. Traces of genomic DNA were removed by treatment with Dnase I (Roche). RNA was purified by phenol/chloroform extraction and precipitated with isopropanol. RT-PCR was performed with the Superscript One-Step RT-PCR Kit with Platinum Taq (Invitrogen). The primer sequences for each human target gene were as follows: apelin, sense (5′-GGG GGA AGC AGG CAG TGA GAA G-3′) and antisense (5′-GAA TGG GCT GGA AGC GGC AAT GT-3′); APJ, sense (5′-CTG GCT GTA GGG GAT GGA TTT CTC-3′) and antisense (5′-CAC CGG GGA CTT GGA GAA CAC C-3′); and GAPDH, sense (5′-CAT GTG GGC CAT GAG GTC CAC CAC-3′) and antisense (5′-TGA AGG TCG GAG TCA ACG GAT TTG GT-3′). The reverse transcription was carried out at 50 °C for 30 min using 500 ng of total RNA. The PCR conditions were as follows: denaturation at 94 °C for 15 s, annealing at 58.9 °C for human APJ and human GAPDH and 61.1 °C for human apelin for 30 s and extension at 72 °C for 2 min. 40 cycles were carried out followed by an extension step at 70 °C for 7 min. The expected amplification products of 300, 600 and 960 bp for apelin, APJ, and GAPDH, respectively were examined on a 2% agarose gel.

For quantitative real-time PCR, total RNA was prepared from HUVEC (3rd passage) and HUAEC (5th passage) using the RNeasy Mini Kit (Qiagen). First strand cDNAs were synthesized using random hexamer primers and TaqMan Reverse Transcription Reagents (Applied Biosystems). For each cell type, 100 ng cDNA was analyzed by real-time PCR using the following TaqMan Gene Expression Assays (Applied Biosystems): Apelin (Assay ID: Hs00936329_m1), APJ (Hs00945496_s1), and GAPDH (Hs99999905_m1). TaqMan PCR was done with an ABI 7900HT Real-Time PCR System (Applied Biosystems). The relative expression levels of apelin and APJ were normalized to the amount of the house keeping gene GAPDH in the same cDNA preparation.

Cell proliferation assays

A colorimetric method measuring conversion of the MTS tetrazolium compound to a water-soluble formazon dye, which is proportional to the number of metabolically active cells, was used to assay cell proliferation (Cory et al., 1991). Primary endothelial cells were seeded into 96-well plates (1500 cells/well) in 150 μl minimal medium (EBM-2, Cambrex; 1% FCS, GIBCO; 0.1% BSA) containing 50 μg/ml gentamicin. After overnight incubation at 37 °C, the medium was supplemented with VEGF165, bFGF or apelin-13. VEGF and bFGF were used at their optimal concentration of 1 and 10 ng/ml, respectively, as determined in pilot experiments (data not shown). Apelin-13 was used in concentrations ranging from 0.1 to 100 nM. Fresh minimal medium containing the growth factors was added every 24 h. Control wells were treated identically using minimal medium without growth factors. After 72 h, cell proliferation was measured using a tetrazolium compound-based [3-(4,5-dimethyl-2-yl)-5-(3-carboxymethoxyphenyl)-2-(4-sulfophenyl)-2H-tetrazolium, inner salt; MTS] assay (CellTiter 96 AQ One Solution Cell Proliferation Assay; Promega) according to the manufacturers instructions. The colorimetric method determines the number of viable, metabolically active cells in culture. 490-nm absorbance was measured using a VersaMax microplate reader (Molecular Devices). Background absorbance from wells containing no cells was subtracted from all measurements and six replicate samples were used to calculate the mean (±standard deviation) in each experiment.

Chemotaxis assays

The chemotactic response of HUVECs was assayed using a 48-well chemotaxis chamber (Neuro Probe, Inc.). Polycarbonate membranes (8-μm pore size; Neuro Probe) were precoated overnight with a 0.1% gelatin solution. Cells were (8×10^5 cells/ml) in minimal medium (EBM-2, 0.1% BSA). Minimal medium without additional factors or containing VEGFA165 (#354107, BD Biosciences), bFGF (#354060, BD Biosciences), apelin-13, or angiotensin II was placed in the lower chambers. 100 μl of cell suspension was added to the upper chamber. After 4 h at 37 °C, non-migrating cells were removed from the upper surface of the membrane and migrated cells on the lower surface were fixed with 100% methanol containing 1 μg/ml DAPI. The stained cells were observed with a fluorescence microscope and digital images of at least seven different fields of the membrane were analyzed using NIH image 1.63 software to assess the number of cells that had migrated. The data shown represent the mean (with a 95% confidence interval) of six independent experiments.

Endothelial spheroid sprouting assay

Endothelial spheroids comprised of 1200 cells were generated as described (Korff and Augustin, 1998). Typically, 40 spheroids were resuspended in 1 ml of a rat tail collagen solution (#1179179, Roche) containing either buffer only, 10 ng/ml VEGF, or 100 nM apelin-13. After 48 h, the number of sprouts per spheroid was quantified using an inverted microscope (Zeiss Axiovert S100 TV).

Analysis of tumor specimens

Formalin-fixed and paraffin-embedded biopsy samples of glioblastoma multiforme (GBM; $n=24$, patients ranging from 37 to 81 years, three of them with an oligodendroglial component) and a control CNS specimen were obtained from the Institute of Neuropathology, University Hospital Zurich, Switzerland. The study was conducted according to the standard regulations of the local ethical committee. The diagnoses of GBM were made in line with the World Health Organization (WHO) classification of brain tumors (Kleihues et al., 2002), and all samples were re-evaluated by FLH. GBMs are defined as malignant astrocytomas displaying tumor necroses and/or microvascular proliferation, and correspond to a WHO grade IV.

Specimens were automatically processed on a Ventana Discovery instrument (Ventana Medical Systems) according to the manufacturer's instructions (Nitta et al., 2003). Briefly, paraffin sections were automatically deparaffinized, fixed, cooked in Tris buffer (pH 6.0) for 60 min and subjected to protease digestion. Hybridizations were performed with digoxigenin-labeled probes (for PECAM1 and VEGF, 5 ng/slide; apelin and APJ, 50 ng/slide) for 6 h, and the signal was detected using a Nitro blue Tetrazolium chloride 5-Bromo-4-cloro-3-indolyl phosphate toluidine salt (NBT/BCLIP) substrate solution for 3 h on the instrument. Digoxigenin-labeled antisense probes were generated from the following plasmids: human APJ (GenBank Acc. No. BI548627), APELIN (BM811482), PECAM1 (BQ067751), and VEGFA (BU153227). Sense probes only exhibit unspecific background signals (not shown).

Photography and computer graphics

Images of cultured cells or sectioned embryos were captured with an AxioCam Colour camera mounted on an Axioscop 2 MOT light microscope (Zeiss) and for whole mount embryo images using a Stemi 2000 stereoscopic microscope (Zeiss). Composite figures were organized and labeled using Adobe Photoshop CS and Adobe Illustrator CS software.

Results

Cloning of Xenopus apelin and APJ cDNAs

We identified two classes of apelin cDNAs, which are derived from two distinct apelin genes, apelin-a and apelin-b, present in the pseudotetraploid *X. laevis* genome (Supplementary Fig. 1). The two genes encode identical polypeptides of 76 amino acids and thus will be referred to as *Xenopus* apelin. Interestingly, the highest degree of amino acid conservation between *Xenopus* and mammals is localized to the C-terminus with a stretch of 14 identical residues harboring apelin-13, the most bioactive apelin peptide (Fig. 1A, Supplementary Fig. 1). We also identified two distinct classes of transcripts encoding *Xenopus* homologues of the apelin receptor APJ, which represent pseudoallelic orthologues and will be referred to as *Xenopus* APJa and APJb (Supplementary Fig. 2). Noteworthy, the *Xenopus* APJa protein is largely identical to the previously reported *Xenopus* Msr protein (Devic et al., 1996), but the two sequences differ with regard to their C-termini due to a single nucleotide insertion in the Msr sequence (Supplementary Fig. 2). The C-termini of the *X. laevis* APJ proteins reported here are identical with the *Xenopus tropicalis* APJ protein (GenBank Acc. No. NM_001032321).

Apelin expression preceeds intersomitic vein angiogenesis

The vascular expression patterns of *Xenopus* APJa (not shown) and APJb (Figs. 1B–E) were identical, in line with the previous report by Devic et al. (1996). Interestingly, apelin expression was strongly upregulated in mesenchymal tissues, which were in close proximity to subsets of newly forming blood vessels (Figs. 1F, G; Supplementary Fig. 3). Particularly, the development of intersomitic vessels, which are the first blood vessels of the embryo to form by sprouting angiogenesis (Poole and Coffin, 1989), was associated with apelin expression (Figs. 1F–I). In *Xenopus*, intersomitic vein (ISV) formation along the anteroposterior body axis occurs in a recurring pattern (Helbling et al., 2000; Millard, 1949). Most strikingly, expression of apelin was detected in cell populations of the dermatome flanking the intersomitic space between trunk somites 2 and 3 (Fig. 1G). Subsequently, dermatomal apelin expression appeared successively in more posterior trunk somites and expres-

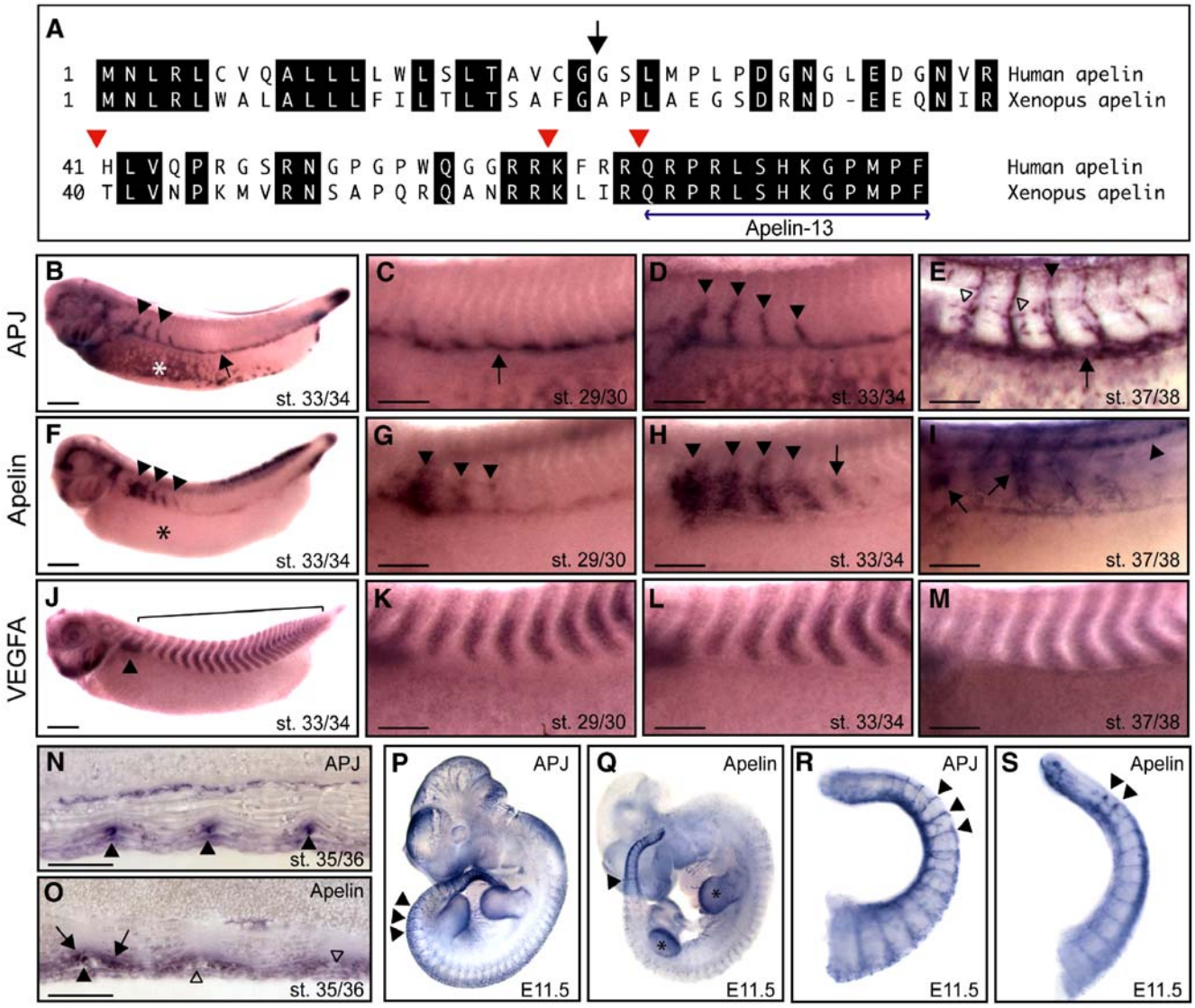

Fig. 1. Apelin expression precedes angiogenic growth of intersomitic vessels. (A) Apelin-13 is conserved from *Xenopus* to man. The amino acid sequences were aligned using ClustalW. Invariant residues are shaded *black*. The conserved, mature apelin-13 peptide is underlined. The predicted sites for signal peptide cleavage (arrow) and proprotein processing (arrowheads) generating apelin-36, apelin-17 and apelin-13 are indicated. (B–S) The expression patterns of apelin and APJ during *Xenopus* embryogenesis (B–O) and in the mouse embryo (P–S) were determined by whole mount *in situ* hybridization. Sections of the trunk (N, O) were cut horizontally at the level of the somites. (B) APJ is detected in all blood vessels including the PCV (arrow), the ISVs (arrowheads) and the VVN (asterisk). (C) APJ is present in the PCV (arrow). (D) Various ISVs (arrowheads) expressing APJ can be detected. (E) APJ levels remain high in all vessels including the ISVs (arrowhead), lateral capillaries (open arrowheads) and the PCV (arrow). (F) Apelin transcripts are found in areas of angiogenesis, such as the intersomitic spaces (arrowheads) but not ventrally (asterisk), where the VVN is forming by vasculogenesis (compare with panel B). (G) In the dermatome (arrowhead), apelin marks the intersomitic spaces, where ISVs will start to sprout. (H) Apelin mRNA is found in areas, where newly forming ISVs are detected (arrowheads). Most notably, a further, posterior domain (arrow) expresses apelin, while no ISV has emerged yet (compare with panel D). (I) Apelin stains the dorsal neural tube (arrowhead) and lateral capillaries (arrows) sprouting into the somites. (J) VEGFA is expressed in all somites (bracket) and the pronephric glomerulus (arrowhead). (K, L) Somitic VEGFA expression remains unaltered during intersomitic vessel growth. (M) Downregulation of VEGFA as ISV formation is completed. (N) APJ staining is confined to the ISVs (arrowheads). (O) Apelin stains the dermatome flanking the intersomitic spaces (arrows). The most mature ISVs express apelin (arrowhead), while the others are still negative (open arrowheads). (P) APJ is expressed throughout the developing vasculature including intersomitic vessels (arrowheads). (Q) Apelin expression is restricted to tissue undergoing angiogenesis, such as the tail (arrowhead) and limb buds (asterisks). (R) Tail explant, where APJ expression is detected in all intersomitic vessels (arrowhead). (S) Apelin stains intersomitic vessels, particularly in the leading edges (arrowheads).

sion always preceded the initiation of novel ISVs (compare Figs. 1C–E with G–I). As revealed by sectioning, intersomitic veins start expressing apelin as they extend (Figs. 1N, O). This suggests that apelin acts initially in a paracrine manner and subsequently in an autocrine fashion to stimulate APJ signaling in intersomitic endothelia. Apelin expression is also associated with mesenchymal tissues in other areas of angiogenic blood vessel growth, such as the head, the visceral arches, and the dorsal midline (Fig. 1F; Supplementary Fig. 3). Expression is, however, notably absent from the vitelline vein network (VVN), which is generated by vasculogenic mechanisms (Figs. 1B, F). In mouse embryos, high levels of APJ expression were detected

in all vascular beds of the body including the eyes and developing limbs (Figs. 1P, R; Supplementary Fig. 4), in line with earlier reports (Devic et al., 1999; Saint-Geniez et al., 2002). In contrast, apelin expression was restricted to areas of ongoing angiogenesis, such as intersomitic spaces, the dorsal midline, and limb buds (Figs. 1P, S; Supplementary Fig. 4). Hence, apelin and APJ expression during angiogenesis is conserved between vertebrates.

Apelin signaling is induced during tumor angiogenesis

We next asked whether apelin and APJ are expressed in human brain tumors presenting with extensive vessel formation. To date, 24 glioblastoma multiforme (GBM) specimens were analyzed (Fig. 2). GBM is typically composed of poorly differentiated neoplastic astrocytes and characterized by increased cell proliferation, tumor necrosis, and extensive angiogenesis (Kleihues et al., 2002). Expression of the endothelial marker PECAM1 (CD31) identified intraparenchymal and meningeal vessels within normal tissue of the central nervous system (Fig. 2G). Microvascular proliferations, sometimes presenting as multilayered 'glomeroid tuft' within GBM specimens, appeared to display a stronger PECAM1 signal when compared to normal controls (Fig. 2B). While VEGFA and apelin were undetectable in normal brain vessels, APJ exhibited low-level RNA expression (Figs. 2H–J). However, APJ and apelin transcripts were consistently highly upregulated within microvascular proliferations in GBM specimens ($n=24$; Figs. 2D, E). In addition, apelin and APJ transcripts (Figs. 2C–E) – albeit less pronounced when compared to microvascular proliferations – were preferentially expressed in radially orientated neoplastic cells surrounding band-like or serpiginous necrotic foci ("pseudopalisading necroses"). These observations are reminiscent of PDGF and VEGF expression patterns, as previously described (Hermanson et al., 1992; Plate and Risau, 1995).

Apelin signaling is required for intersomitic vein angiogenesis

We performed loss-of-function studies in *Xenopus* embryos using morpholino antisense oligonucleotides (MO) to assess the

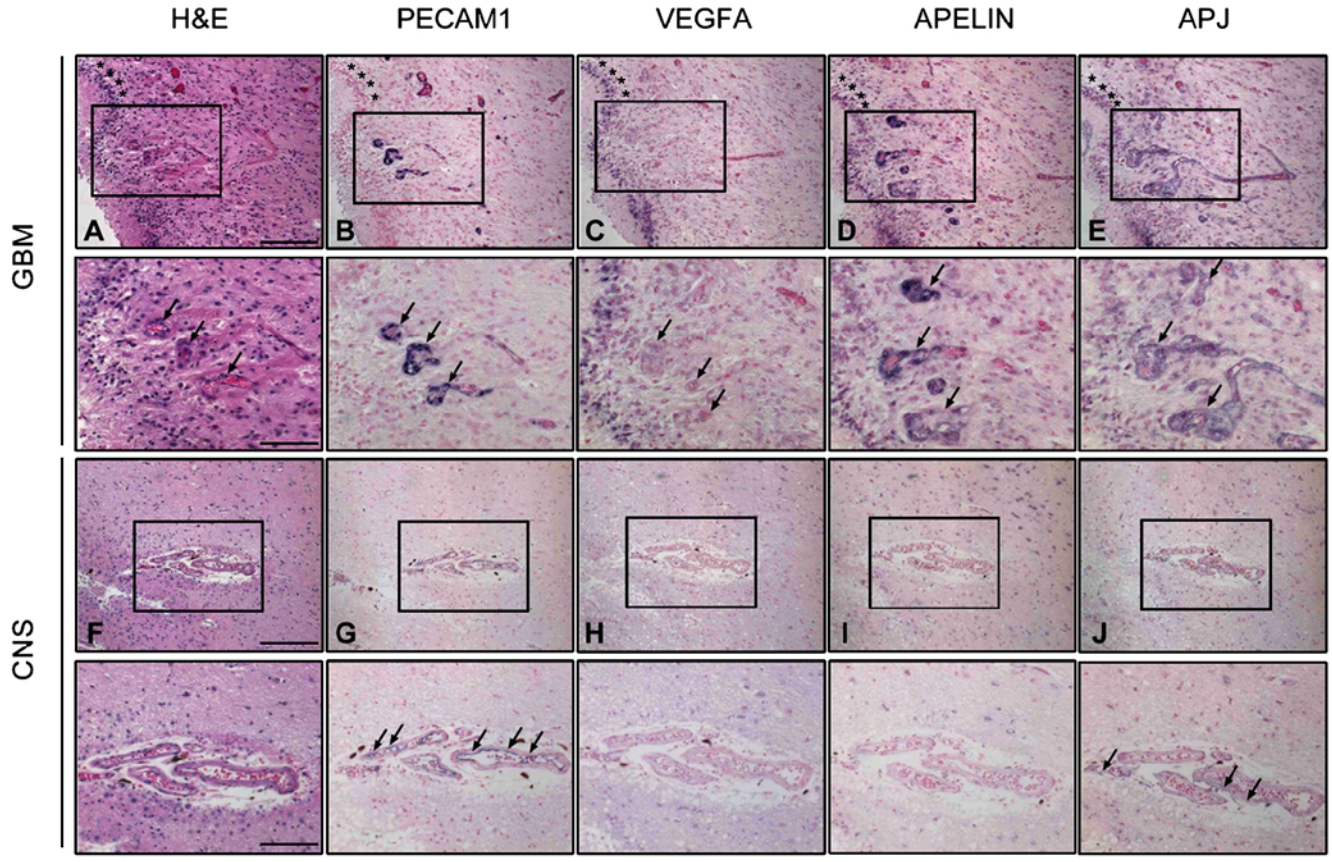

Fig. 2. Apelin and APJ are upregulated in GBM specimens. Sections of GBM specimens and of normal CNS tissue were stained with hematoxylin and eosin (H&E) or used for *in situ* hybridization. Close-up views of the boxed areas are shown below each panel. Pseudopalisading necroses are indicated with asterisks. Scale bars: 200 μm (A–J), 100 μm (close-up views). (A) H&E staining of GBM specimen. (B) Glomeruloid tuft-like microvascular proliferations (arrows) of GBM are positive for PECAM1 expression. (C) Radially orientated neoplastic cells surrounding band-like necroses (asterisks) express VEGFA. Baseline VEGFA expression is also seen in microvascular proliferations (arrows). (D) High-level of APELIN expression is detected within microvascular proliferations (arrows) and, to some extent, within radially orientated neoplastic cells surrounding band-like necroses (asterisks). (E) APJ is upregulated within microvascular proliferations (arrows) and occasionally within neoplastic cells accumulating next to band-like necroses (asterisks). (F) H&E staining of normal CNS tissue specimen. (G) Meningeal (arrows) as well as intraparenchymal vessels (not shown) within normal CNS tissue display PECAM1 signals. (H, I) VEGFA (H) and APELIN (I) expression is undetectable in vessels of normal CNS tissues. (J) Moderate APJ staining (arrows) is present in meningeal vessels of normal CNS tissue.

role of APJ and apelin in vertebrate blood vessel development. Special care was taken to select MOs, which target transcripts of both pseudoallelic genes (Supplementary Figs. 1 and 2). Furthermore, mispaired MOs were used as specificity controls. The MOs inhibited protein synthesis in cell-free coupled transcription–translation assays (Supplementary Fig. 5).

MO-injected embryos were analyzed by *in situ* hybridization using a collection of tissue-specific molecular markers to visualize the developing vasculature (Fig. 3A, Supplementary Fig. 6; data not shown for Tie2, VEGFR1, VEGFR2). Neither injection of apelin-MO nor APJ-MO resulted in alteration of the general expression levels and domains of apelin (Supplementary Fig. 6) and APJ (not shown). This indicates that the expression of apelin and APJ is not subject to autoregulation. Marker gene analysis of MO-injected embryos indicated that development of erythrocytes, pronephric kidneys, somites, and the nervous system was unperturbed (Supplementary Fig. 6; not shown). The assembly of the primary vascular plexus consisting of the VVN and associated major vessels such as the posterior cardinal veins (PCV) appeared unaffected (Fig. 3A; Supplementary Fig. 6). We therefore conclude that apelin-APJ signaling is not required for vasculogenesis.

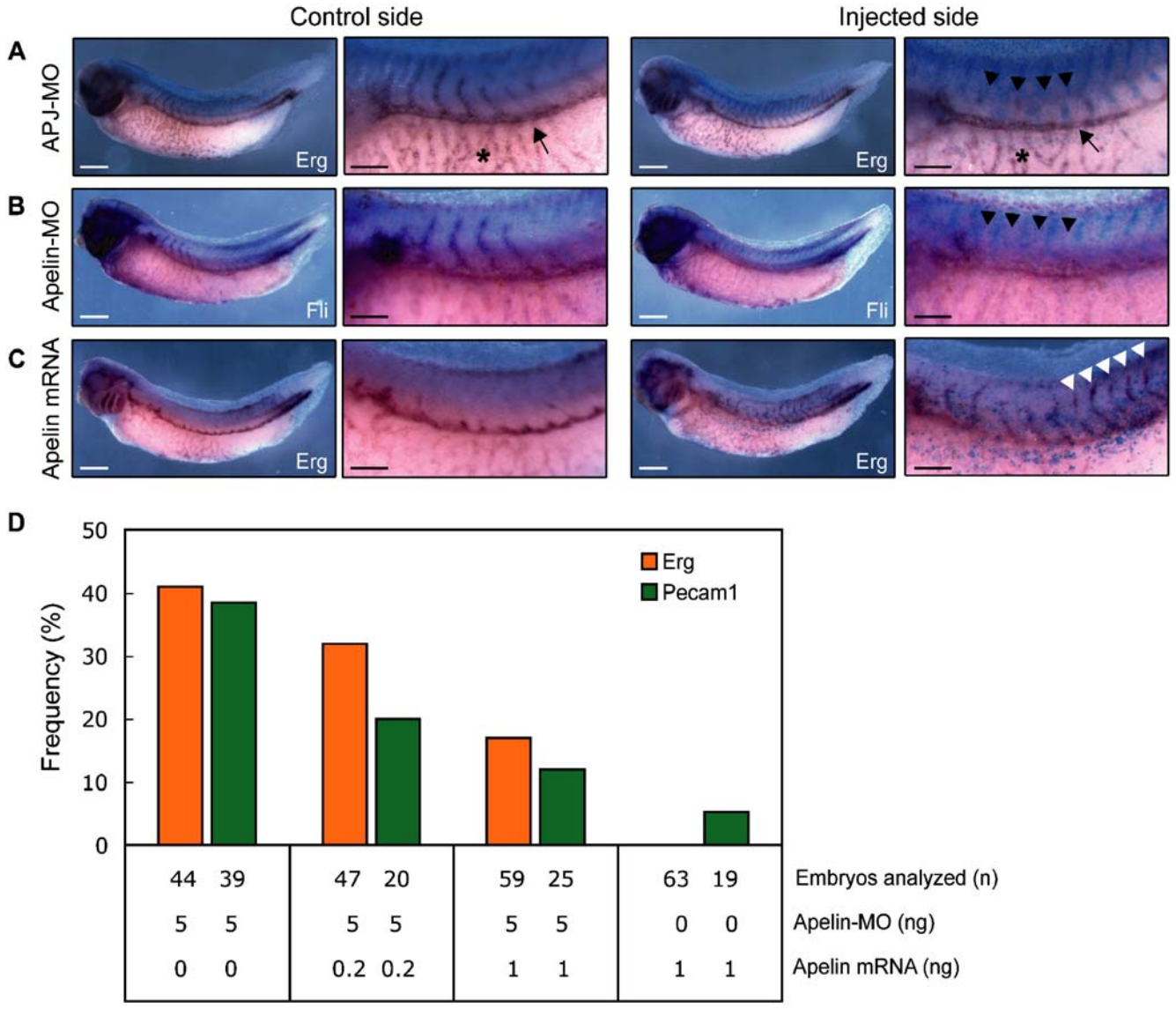

Fig. 3. Apelin-APJ signaling is necessary and sufficient for ISV angiogenesis. MO oligonucleotides (5 ng) or apelin mRNA (1 ng) and mRNA (0.25 ng) for the lineage tracer nuclear β-gal were co-injected into single blastomeres. Injected embryos were raised to stage 32 (C), 35/36 (A, B) or stage 37/38 (D), fixed, and processed for β-gal activity. Expression of marker genes was visualized by *in situ* hybridization. Scale bars: 400 μm, embryo views; 200 μm, close-up views. (A, B) APJ and apelin are required for ISV angiogenesis. Arrowheads indicate the intersomitic spaces, which are devoid of ISVs. Note that the PCV (arrow) and the VVN (asterisk) remain unaffected. (C) Apelin is sufficient to induce premature angiogenesis of ISVs. Single V2 blastomeres of 8-cell-stage embryos were injected with apelin mRNA (1 ng). On the injected side, all intersomitic spaces including the posterior ones (white arrowheads) are occupied by ISVs, which had formed prematurely. Note that at stage 32, the control side is largely devoid of ISVs. (D) Co-injection of apelin mRNA rescues the apelin-MO phenotype. The indicated amounts of MOs and/or mRNA were injected unilaterally into single blastomeres of 2-cell stage embryos. ISVs were visualized *in situ* hybridization, and the frequencies of embryos with severe ISV defects were determined.

In contrast, we found that the formation of ISVs was profoundly affected by MO injections (Figs. 3A, B; Table 1). ISV growth was impaired by injection of either apelin-MOs or APJ-MOs. Similarly, co-injection of both apelin- and APJ-MOs caused ISV phenotypes. Rescue experiments revealed substantial, dose-dependent restoration of the ISV growth by prepro-apelin mRNA (Fig. 3D). In an alternative approach, we also evaluated whether a recently described apelin-specific antagonist (Lee et al., 2005), apelin-13 (F13A), would interfere with ISV formation *in vivo*. In contrast to apelin-MO knockdowns, injections of *Xenopus* apelin-13 (F13A) mRNA failed to disrupt ISV formation in a dominant manner (not shown). Our findings support previous studies indicating that apelin-13(F13A) does not act in an antagonistic manner (Fan et al., 2003; Medhurst et al., 2003). Taken together, the MO knockdown experiments demonstrate that both apelin and its receptor APJ are dispensable for vasculogenesis but are required for angiogenesis of ISVs.

Apelin is sufficient to induce premature intersomitic vein angiogenesis

As shown in Fig. 1, the expression of apelin is temporally and spatially highly regulated and precedes the initiation of ISV growth. We therefore asked whether premature, ectopic expression of apelin in the developing somites would have an effect on intersomitic vessel formation. Injections of apelin mRNA were performed unilaterally into single V2 blastomeres at the 8-cell stage. The injected embryos were raised until stage 32, when the control sides showed evidence for the initiation of the most anterior ISVs (Fig. 3C). By contrast, injection of apelin induced fully extended ISVs. This phenotype was observed by using different molecular markers, such as Erg (Fig. 3C), VEGFR2 and Pecam1 (not shown) in repeated experiments ($N=4$), and occurred on average in about 57% of the apelin-injected embryos (range 42–82%; $n=110$). Remarkably, there was no evidence for mistargeting of the prematurely formed ISVs indicating that EphB4-mediated repulsive signaling (Helbling et al., 2000) was fully functioning. Overexpression experiments with APJ mRNA did not result in abnormal or premature vascular development (not shown). We conclude that ectopic apelin expression alone is sufficient to induce premature angiogenesis of ISVs in *Xenopus*.

Table 1
Summary of intersomitic vein defects in MO-injected *Xenopus* embryos

Injected MO	Amount of MO injected (ng)	Average frequency of embryos with ISV defects (%)	Total number of embryos analyzed (*n*)
Apelin-MO	5	49	239
Apelin(mp)-MO	5	2	175
APJ-MO	5	56	276
APJ(mp)-MO	5	9	139
Apelin-MO and APJ-MO	5 5	63	95

MO injections were performed unilaterally into single blastomeres at the two cell-stage. At stage 35/36, embryos were processed for whole mount *in situ* hybridization. The vascular marker Erg was used to visualize ISVs. The embryos were scored for strongly reduced and/or absent ISVs. For each MO, two to eight independent experiments were performed. Similar results were obtained with embryos stained for the vascular markers VEGFR2 and APJ. ISV, intersomitic vein; MO, morpholino; mp, mispaired control.

VEGFA is not sufficient to trigger premature intersomitic vein angiogenesis

To explore the epistatic relationship between VEGFA and apelin signaling in ISV angiogenesis, we first compared the temporal and spatial expression of VEGFA to apelin. We identified a novel *Xenopus* VEGFA isoform, VEGFAb168, which is equivalent to human VEGFA165, transcript variant 4 (Supplementary Fig. 7). *Xenopus* VEGFAb168 is derived from a second pseudoallelic *X. laevis* VEGFA gene, VEGFA-b. The two *Xenopus* VEGFA genes are expressed in an identical fashion. Somitic expression of VEGFA is detected as early as stage 23 (Cleaver et al., 1997) prior to apelin expression, which is only detectable from stage 29/30 onwards (Figs. 1G, K). Importantly, VEGFA expression is present simultaneously in all developing somites and is gradually downregulated at stage 37/38 (Figs. 1J–M). On the contrary, apelin expression is intimately correlated with the appearance of ISVs along the anteroposterior body axis (Figs. 1F–I).

To assess whether apelin and APJ expression requires VEGFA signaling, we injected VEGFA-MOs (Supplementary Fig. 7). Knockdown of VEGFA caused severe vascular abnormalities including absence of ISVs, defects in PCV assembly, and development of an immature, hypoplastic VVN (Fig. 4A; Supplementary Fig. 5; Table 2). This indicates that VEGFA is required for vasculogenesis in *Xenopus*. Interestingly, expression of APJ and apelin was unaffected in VEGFA-MO injected embryos (not shown). This suggests that VEGFA signaling does not initiate vascular APJ and somitic apelin expression.

Unilateral injections of VEGFA mRNA failed to promote premature outgrowth of ISVs, but caused severe disorganization of the VVN (Fig. 4B). The characteristic, highly elaborate VVN pattern (Fig. 4A, control side) had collapsed into a disorganized and hyperplastic structure, where distinct vessels were no longer discernable. This VVN phenotype is clearly different from the one seen in VEGFA knockdown embryos (compare Figs. 4A, B). Notably, we frequently observed the VVN phenotype bilaterally indicating that the injected VEGFA mRNA acted at long range (Fig. 4B). Unlike control embryos, most hyperplastic VVNs of the VEGFA-injected embryos (85%, $n=39$) expressed apelin ectopically (Figs. 4C, H). Hence, in contrast to apelin, VEGFA was not sufficient to promote premature ISV angiogenesis. VEGFA overexpression was, however, sufficient to induce ectopic apelin expression in the VVN. Since VEGFA is not required for apelin expression, multiple signaling pathways may act along side of VEGFA to induce and/or maintain apelin expression.

VEGFA acts upstream of apelin in vascular development

We performed combinations of gain- and loss-of-function experiments to further explore the epistatic relationship of

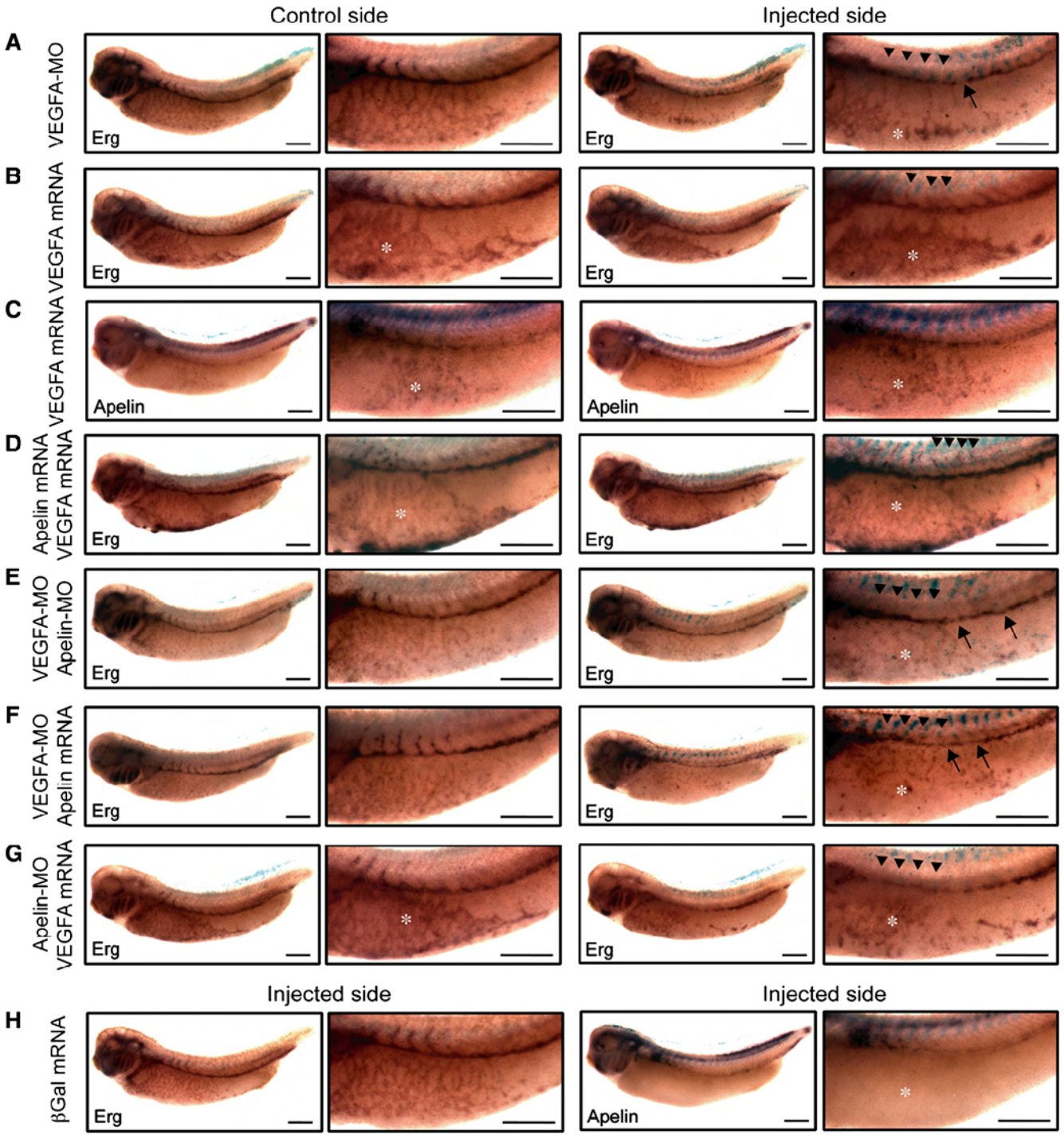

Fig. 4. VEGFA acts upstream of apelin signaling in vascular development. MO oligonucleotides and/or mRNA were co-injected unilaterally into single D2 (A, B, D, F) or V2 (C, E, G, H) blastomeres of 8-cell stage embryos. Injected embryos were raised to stage 35/36 and processed *in situ* hybridization. (A) The vascular defects in VEGFA-MO (5 ng) injected embryos included defective assembly of the PCV (arrow), absence of ISVs (arrowheads) and hypoplasia of the VVN (asterisk). (B) Overexpression of VEGFA (1 ng mRNA) did not affect ISV formation (arrowheads) but caused hyperplasia of the VVN (asterisks). Note that the VVN defects occur bilaterally. (C) Overexpression of VEGFA (1 ng mRNA) induces widespread, bilateral ectopic expression of apelin (asterisks) in the ventral belly (compare with H, right panel). (D) Co-injection of VEGFA and apelin mRNA (0.5 ng each) results in VVN hyperplasia (asterisk) and premature outgrowth of ISVs (arrowheads). (E) Double-knockdown of VEGFA and apelin results in vascular defects comparable to panel A. (F) Apelin mRNA (1 ng) fails to rescue vascular development in VEGFA-MO (5 ng) injected embryos. The resulting embryos lack ISVs (arrowheads), have PCV defects (arrows) and display a hyperplastic VVN (asterisk). (G) VEGFA mRNA (1 ng) fails to rescue the ISV defects in apelin-MO (5 ng) injected embryos. Embryos lack ISVs (arrowhead) and display bilateral VVN hyperplasia (asterisk). (H) Injection of β-gal mRNA (1.25 ng) has no effect on vascular development and apelin expression. Note the lack of apelin expression (asterisk) in the ventral belly.

Table 2
Summary of vascular phenotypes of mRNA and MO-injected embryos

Injected reagents	Amount of injected reagent (ng)	Injected blastomere	Average frequency of embryos with the indicated vascular defect (%)			Number of embryos analyzed (*n*)
			VVN defects	Premature ISVs	Loss of ISVs	
VEGFA-MO	5	D2	70 [a]	0	91	23
VEGFA RNA	1	D2	89 [b]	0	0	65
VEGFA RNA and apelin RNA	0.5 0.5	D2	89 [b]	61	0	46
VEGFA-MO and apelin RNA	5 1	D2	89 [a]	0	59	61
VEGFA RNA	1	V2	94 [b]	7	0	118
Apelin-MO	5	V2	0	0	71	65
Apelin-MO and VEGFA RNA	5 1	V2	98 [b]	0	52	84

MO and/or mRNA injections were performed unilaterally into single blastomeres of 8-cell stage embryos as indicated. The vascular phenotypes were scored in stage 32 embryos stained for expression of the vascular marker Erg. Each experiment was performed at least twice. Similar results were obtained with embryos stained with the vascular markers VEGFR2 and APJ. VEGFA RNA and apelin RNA refer to VEGFAb168 and preproapelin mRNA injections, respectively. ISV, intersomitic vein; MO, morpholino; VVN, vitelline vein network.

[a] Frequency of hypoplastic VVN.

[b] Frequency of hyperplastic VVN.

VEGFA and apelin signaling in vascular development. First, we co-injected VEGFA and preproapelin mRNA. The resulting embryos displayed a combination of two gain-of-function phenotypes, namely (i) disorganized, hyperplastic VVNs and (ii) premature ISV angiogenesis (Fig. 4D). Apelin and VEGFA overexpression have therefore distinct effects on vascular development in *Xenopus* embryos. Interestingly, knocking down both VEGFA and apelin resulted in a severe vasculogenesis phenotype similar to VEGFA-MO-only-treated embryos (compare Figs. 4A, E). We then asked whether injection of preproapelin mRNA could rescue the vasculogenesis phenotype observed in VEGFA knockdown embryos, which was however not the case (Figs. 4A, F). Finally, we found that VEGFA did not restore ISV outgrowth in apelin knockdown embryos (Fig. 4G). Collectively, VEGFA acts prior to apelin in ISV angiogenesis.

Xenopus APJ mediates apelin signaling

We performed *in vitro* studies to address whether apelin-13 induces internalization of *Xenopus* APJ and activation of signaling. Fusion of the enhanced version of green fluorescent protein (EGFP) to mammalian APJ proteins does not interfere with receptor functions (Reaux et al., 2001; Zhou et al., 2003). Therefore, a CHO cell line was established expressing a *Xenopus* APJ-EGFP fusion protein and ligand-induced internalization of *Xenopus* APJ was monitored by confocal fluorescence microscopy. In the absence of apelin, APJ primarily localized to the cell surface (Fig. 5A). After exposure to apelin-13, the receptor was redistributed to the cytoplasm with distinct perinuclear accumulation. In contrast, the localization of APJ was not altered by addition of angiotensin II (not shown). Apelin signaling inhibits forskolin-induced cAMP production, which indicates that APJ couples to inhibitory G-proteins G_i (Habata et al., 1999). Similarly, cAMP production was inhibited in CHO cells expressing *Xenopus* APJ by apelin-13. The inhibition was dose-dependent with a half-maximal inhibition IC50 value of 45 (±15) nM (Fig. 5B). Taken together, our findings demonstrate that *Xenopus* APJ is a genuine receptor for apelin-13.

Apelin elicits a chemotactic response in primary human endothelial cells

It previously has been reported that apelin stimulates proliferation and migration of RF/6A cells, a rhesus macaque

Fig. 5. Apelin-13 activates signaling of *Xenopus* APJ and promotes chemotaxis of primary human endothelial cells. (A) Induction of *Xenopus* APJ internalization by apelin-13. Confocal images of DAPI (blue) stained CHO cells expressing *Xenopus* APJ-EGFP (green) before (control) and 30 min after addition of 100 nM apelin-13 are shown. Scale bar, 10 μm. (B) Activation of *Xenopus* APJ signaling by apelin-13. Dose–response curves of the inhibition of cAMP production in CHO-APJ (*blue*) and the parental CHO (*red*) cell line in the presence of 0.2 mM IBMX and 1 μM forskolin are shown. The inhibition of cAMP production is indicated as the percentage of inhibition against maximum cAMP production by cells without apelin treatment. The values represent mean (±S.D.) of triplicate assays. (C) Comparison of the apelin and APJ expression levels in primary endothelial cells analyzed by quantitative real-time PCR (upper panel) and RT-PCR (lower panel). Upper panel: The expression levels are expressed as arbitrary units normalized to GAPDH, and are the mean (±S.D.) of triplicates. Lower panel: RT-PCR analysis was performed in presence (+) or absence (−) of reverse transcriptase. (D) Cell proliferation assays performed with HUVECs in presence of different factors. The cells were incubated for 72 h with the indicated polypeptides. Cell proliferation was measured using a MTS-based colorimetric assay. The obtained proliferative responses are represented as percentage of increase of absorbance against control cells. The results are shown as the mean (±S.D.) of 6 biological replicates. **P*-value < 0.01 vs. control by one-way ANOVA. (E) Induction of chemotaxis in HUVECs by apelin-13. Chemotactic responses are indicated as the increase in percentage of cells migrating towards the chemokine gradient against control cells without treatment. **P*-value < 0.001 vs. control by one-way ANOVA. (F) Endothelial spheroid vessel outgrowth after VEGFA and apelin treatment. Collagen-embedded HUVEC spheroids were incubated with VEGFA (10 ng/ml; 0.5 nM) or apelin-13 (100 nM) for 48 h. The number of sprouts from at least 14 spheroids was quantified and is given as mean±S.D. Scale bars, 100 μm.

choroid-retina-derived endothelial cell line (Kasai et al., 2004). However, RF/6A cells are spontaneously immortalized cells and may therefore differ from primary endothelial cells in their responses to apelin. Hence, we tested primary human endothelial cells for expression of apelin and APJ. For human umbilical vein endothelial cells (HUVEC), expression of apelin has been previously demonstrated (Kasai et al., 2004); however, it is still a matter of debate whether HUVECs express APJ constitutively (Kasai et al., 2004; Masri et al., 2004). We tested HUVEC and human umbilical arterial endothelial cells (HUAEC) by

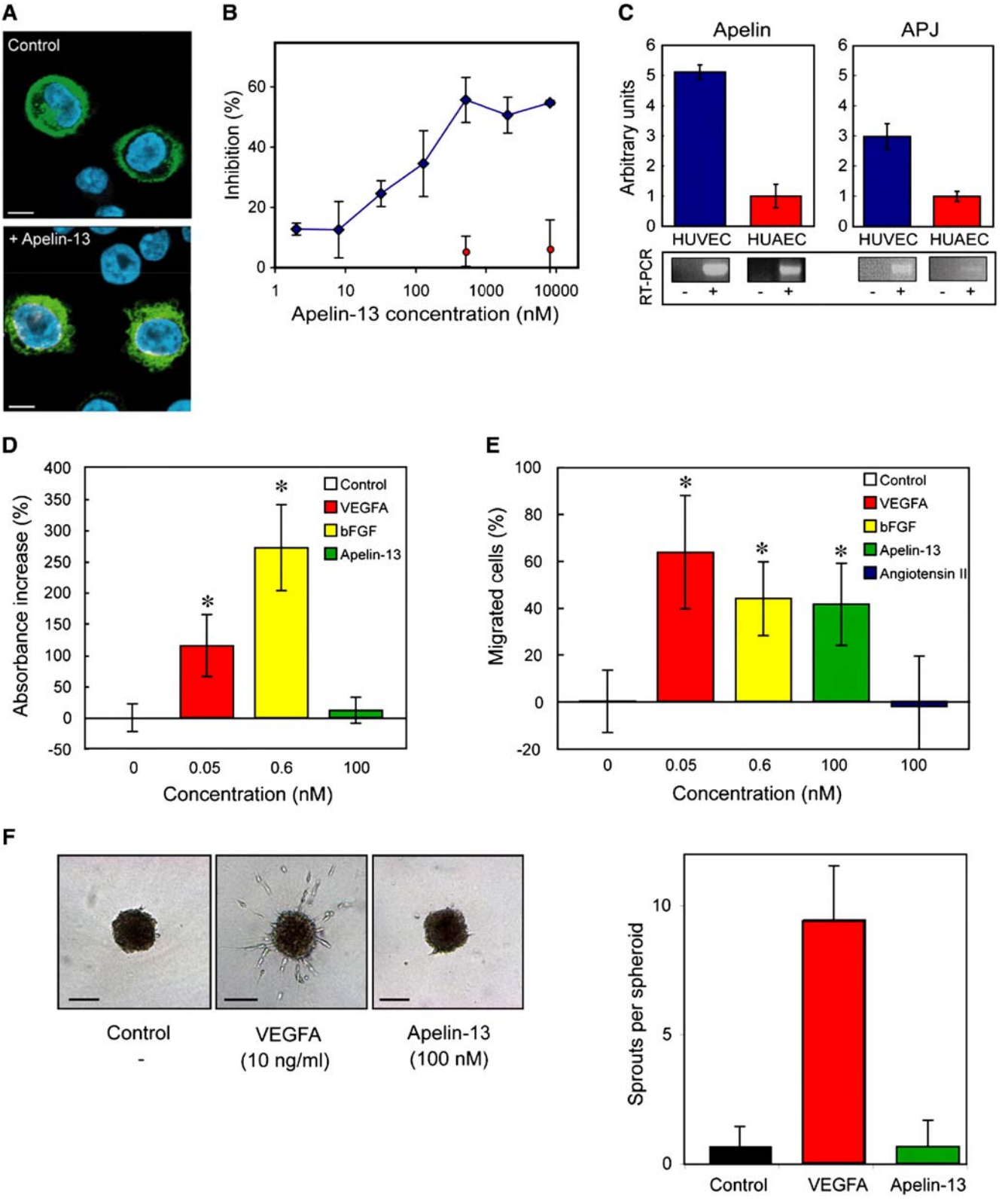

conventional RT-PCR as well as quantitative real-time PCR for expression of apelin and APJ. Interestingly, the relative expression levels of APJ and apelin were 3- and 5-fold, respectively, in HUVECs over HUAECs. Finally, we also assessed human dermal microvascular endothelial cells (HMVEC-D). Here, quantitative PCR revealed apelin and APJ expression at levels similar to HUVECs and HUAECs, respectively (not shown). Since HUVECs expressed highest levels of APJ mRNA, they were used in all subsequent cell-based assays.

The proliferative response of serum-starved HUVECs to apelin treatment was compared to VEGFA165 and basic FGF (bFGF), two potent endothelial cell mitogens (Esch et al., 1985; Keck et al., 1989; Leung et al., 1989). As expected, treatment of HUVECs with VEGFA165 or bFGF within 72 h caused a robust mitogenic response. In contrast, apelin-13 (0.1 to 100 nM were tested) neither induced significant proliferation of HUVECs nor did it cause detectable cell death (Fig. 5D). Similar results were obtained with HUAECs and HMVEC-Ds (not shown). We therefore conclude that primary human endothelial cells, unlike immortalized endothelial cells, do not show a significant proliferative response to apelin-13.

Next, we determined whether apelin-13 may confer chemoattraction to primary endothelial cells. As shown in Fig. 5E, stimulation with apelin-13 led to a 40% increase in directed migration of HUVECs across semi-permeable membrane supports. Consistent with a previous study (Desideri et al., 2003), angiotensin II did not promote HUVEC migration. The enhancement of cell migration by apelin was comparable to bFGF treatment but not as pronounced as with VEGFA. Finally, we utilized an endothelial cell spheroid assay (Korff and Augustin, 1998; Korff and Augustin, 1999) to assess whether apelin-13 is sufficient to promote angiogenic sprouting *in vitro*. While VEGFA supported robust radial sprouting, apelin-13 treatment failed to induce discernible effects with HUVEC, HUAEC, and HMVEC-D spheroids (Fig. 5F; not shown). Moreover, no synergistic activities were detected, when spheroids were treated both with VEGFA and apelin-13 (not shown). In summary, these results suggest that apelin-13 has no apparent mitogenic activity on primary human endothelial cells nor is it able to induce angiogenic sprouting of spheroid cultures by itself. Apelin-13 acts, however, as a potent chemotactic factor for human endothelial cells.

Discussion

In the present study, we examined the role of the GPCR APJ and its ligand apelin in embryonic and pathologic angiogenesis. Two recent studies have reported contradicting findings on the role of apelin signaling during blood vessel development in *Xenopus* (Cox et al., 2006; Inui et al., 2006). Here we show that apelin-APJ signaling is required for embryonic angiogenesis in *Xenopus*. Furthermore, apelin is sufficient to induce a robust angiogenic response *in vivo*. These findings confirm and extend the recent study of Cox et al. (2006). We also show that apelin acts both via paracrine as well as autocrine mechanisms to promote angiogenesis *in vivo*. Moreover, we demonstrate here that apelin functions as a chemoattractant rather than a mitogen on primary human endothelial cells. Finally, we provide first evidence linking apelin-APJ signaling to tumor angiogenesis in human neoplasms.

Evolutionary conservation of vertebrate apelin proteins

Proteolytic maturation of preproapelin generates the apelin-36, apelin-17, and apelin-13 peptides, where apelin-13 represents the most active isoform (Hosoya et al., 2000; Tatemoto et al., 1998). Since apelin-13 is sufficient to induce full activation of APJ signaling, the physiological significance of the longer isoforms has been unclear. Interestingly, cloning of the *Xenopus* apelin gene revealed that the mature apelin-13 peptide has remained invariant during 360 million years of tetrapod evolution, while the longer apelin-17 and apelin-36 peptides differ considerably. The invariant amino acid residues shared by the longer forms are confined to the predicted proteolytic cleavage sites. Apelin-13 therefore represents the primary, physiologically important protein product of the apelin gene. Given the lack of evolutionary conservation, apelin-36 may function as a precursor with some biological activity until undergoing further proteolysis to yield the fully active apelin-13 peptide.

Apelin expression is confined to areas of embryonic angiogenesis

Earlier studies have shown that APJ is expressed in blood vessels of the developing mouse and *Xenopus* embryo (Devic et al., 1996; Devic et al., 1999). Here, we show that the expression patterns of the APJ ligand apelin are conserved between mouse and *Xenopus*. Apelin expression occurred either in close vicinity to APJ or was coexpressed with APJ in endothelia. Strikingly, apelin expression preceded the onset of ISV growth—a finding previously not reported by others. First, cells of the dermatome flanking the intersomitic space initiate apelin expression. Once the ISV has sprouted, apelin and APJ are coexpressed in the extending intersomitic capillary. Hence, paracrine signaling of apelin acts initially on the newly forming ISV, while subsequent autocrine apelin signaling may sustain extension of ISVs. Autocrine apelin signaling has also been reported in the leading edge of retinal vessels in mice (Saint-Geniez et al., 2002). Furthermore, our data on coexpression of apelin and APJ in different primary human endothelial cell types also implies autocrine signalling activities. Remarkably, both modes of signaling may also operate during tumor angiogenesis (see below) suggesting a general flexibility of apelin signaling mechanisms *in vivo*.

Apelin signaling is necessary and sufficient to trigger embryonic angiogenesis

Contradicting findings regarding the role of apelin signaling during *Xenopus* embryogenesis have been recently reported (Cox et al., 2006; Inui et al., 2006). The loss-of-function studies reported here fully support and extend the observations of Cox et al. (2006). Knockdown of apelin in *Xenopus* embryos

revealed a requirement for apelin signaling in ISV angiogenesis. Moreover, disruption of APJ function impaired ISV formation without causing discernable phenotypes during earlier stages of vascular development. Hence, despite widespread expression during vasculogenesis, endothelial APJ functions are only essential during sprouting angiogenesis in areas that express apelin. In the mouse, APJ has recently been implicated in blood pressure control; however, APJ-deficiency resulted in no obvious defects in vascular development (Ishida et al., 2004). The apparent differences in the requirement for APJ function in vascular development between *Xenopus* and mice may indicate redundancy of apelin receptors in higher vertebrates. In an APJ-deficient background, mice may be able to use APJ-related GPCRs, such as AT1R, to mediate apelin signal during angiogenesis. In *Xenopus*, we failed to detect any expression of AT1R or the related AT2R gene during ISV angiogenesis (V. Dabouras and A. W. Brändli, unpublished observations).

The study of Inui et al. (2006) suggests a much more general role for apelin signaling in cardiovascular development and differentiation, which is not supported by Cox et al. (2006) and our work. We do not know the precise reasons for these discrepancies. In our knockdown studies, we failed to detect any evidence for abnormalities in the differentiation of endothelia, erythrocytes, and pronephric epithelia (see Supplementary Fig. 6). Inui et al. injected typically MO doses ranging from 20 to 40 ng, which exceeds our standard 5-ng doses by up to 8-fold. Finally, the apelin-MO used by Inui *et al.* to target the 5′-UTR of apelin perfectly matches apelin-a but harbors 4 mismatches over the 19 nucleotides that align with the known apelin-b nucleotide sequence (GenBank Acc. No. DQ471853). This may explain why the authors had to inject larger amounts of the apelin-MO to induce a knockdown phenotype in *Xenopus* embryos. The widespread cardiovascular defects reported by Inui *et al.* may therefore be caused by off-target effects resulting from injections of exceedingly high doses of MOs.

The angiogenic potential of apelin has recently been documented by different implantation assays, which include Matrigel plug assays in the mouse, chicken chorioallantoic membrane (CAM) assays, and bead—as well as cell implantation experiments in *Xenopus* embryos (Cox et al., 2006; Kasai et al., 2004). We provide here novel evidence for the angiogenic potential of apelin *in vivo*. Apelin expression occurs in a spatially and temporally regulated manner along the anteroposterior axis preceding the initiation of ISV growth. While ectopic apelin expression resulted in premature angiogenic growth of ISVs, VEGFA overexpression failed to elicit a similar response. Our findings therefore imply that VEGFA and apelin fulfill distinct functions in ISV angiogenesis. Most importantly, expression of apelin appears to be the critical event triggering ISV outgrowth. Taken together, the evidence provided here clearly demonstrates that apelin acts as a potent pro-angiogenic factor *in vivo*.

Apelin has chemotactic properties on primary endothelial cells

Angiogenesis is characterized by a complex cascade of events during which the quiescent endothelial cells of a blood vessel become activated to proteolytically degrade their underlying extracellular matrix, directionally migrate towards angiogenic stimuli, proliferate, and form new capillary networks (Carmeliet, 2000). Given its angiogenic properties *in vivo*, the question arises which of these cellular programs are directly controlled by apelin. We and others (Cox et al., 2006; Kasai et al., 2004) have explored the effects of apelin treatment on cultured endothelial cells and obtained partially conflicting results. The most striking differences relate to the mitogenic potential of apelin.

Treatment of apelin promotes cell proliferation of immortalized endothelial cell lines (Cox et al., 2006; Kasai et al., 2004). To reassess the potential mitogenic activity of apelin, we tried to mimic the *in vivo* situation by utilizing human primary endothelial cell preparations (HUVEC, HUAEC, and HMVEC-D) rather than immortalized endothelial cells. Our analysis of early-passage primary endothelial cell preparations revealed that all cells expressed APJ transcripts. Interestingly, immunocytochemical studies have provided independent evidence for APJ expression in HUVECs (Kleinz et al., 2005). We tested a wide range of apelin-13 concentrations in the presence of minimal medium but failed to detect any significant proliferative responses. We therefore conclude that apelin has no profound mitogenic activity on primary human endothelial cells.

First evidence indicating a role of apelin signaling in stimulating cell migration was obtained with APJ-transfected cell lines (Hashimoto et al., 2005; Hosoya et al., 2000). More recently, chemotactic responses of immortalized endothelial cells to apelin treatment were reported (Cox et al., 2006; Kasai et al., 2004). We have now extended these observations to primary human endothelial cells by demonstrating that apelin induced migration of HUVECs in culture. Interestingly, VEGFA readily induced capillary-like sprouting of endothelial spheroids *in vitro* but apelin failed to do so. This suggests that apelin is not sufficient to trigger all necessary steps of angiogenic sprouting *in vitro*. Apelin primarily act as a chemotactic factor on endothelial cells promoting endothelial cell migration.

Distinct roles for VEGFA and apelin in intersomitic vein angiogenesis

VEGFA is a major regulator of blood vessel formation and function (Ferrara et al., 2003). It coordinately controls proliferation, survival, and migration of endothelial cells during blood vessel development. As shown here, VEGFA knockdown experiments in *Xenopus* resulted in severe vascular abnormalities including defects in PCV assembly, development of an immature, hypoplastic VVN, and absence of ISVs. ISV formation in *Xenopus* is, however, not only dependent on VEGFA but also requires apelin signaling. This raises the question of how VEGFA and apelin cooperate in ISV formation. Our studies provide a first glimpse into the possible mechanisms. Knockdown of VEGFA function did neither affect vascular expression of APJ nor did it interfere with expression of apelin in the dermatome. Ectopic expression of VEGFA is, however, sufficient to induce apelin expression in the VVN. Noteworthy, placental growth factor (PlGF, PGF), a VEGF family member,

has been reported to induce apelin expression in primary capillary endothelial cells (Autiero et al., 2003). Collectively, these findings implicate VEGFs as inducers of apelin expression in endothelial cells.

Our studies of VEGFA and apelin function suggest a molecular pathway for ISV development in *Xenopus* (Fig. 6). Initially, somitic VEGFA signals act along the entire anteroposterior axis on the adjacent endothelia of the PCV to initiate the necessary molecular and cellular processes for angiogenic sprouting. Subsequently, paracrine apelin signaling originating from dermatomal cells of the somites triggers the stage-dependent outgrowth of individual intersomitic vessels along the anteroposterior axis. Similar to retinal angiogenesis (Gerhardt et al., 2003), somitic paracrine VEGFA signaling may now serve two distinct functions: in distal endothelial cells of the intersomitic vessel VEGFA may induce a proliferative response, whereas at the leading edge VEGFA possibly guides cell migration. Autocrine apelin signaling may subsequently stimulate motility of endothelial cells at the leading edge. Finally, repulsive Eph receptor signaling restricts angiogenic growth to the intersomitic spaces as previously demonstrated (Helbling et al., 2000).

Apelin signaling in tumor angiogenesis

The marked induction of angiogenesis in GBMs (Yao et al., 2001) suggests that pathological vessel formation is required for tumor progression. In normal brain tissue, no apelin and only trace amounts of APJ were detectable in meningeal and intraparenchymal blood vessels. By contrast, we consistently found a dramatic upregulation of apelin and APJ expression within GBM-associated microvascular proliferations, particularly in areas of vessel sprouting and branching. Coexpression of ligand and receptor in the angiogenic tumor vasculature is consistent with an autocrine mode of signaling, similar to the developmental regulation of apelin and APJ. Apelin expression was also detectable in radially oriented tumor cells surrounding band-like necrotic foci—a finding which may indicate that apelin, like VEGFA (Plate et al., 1992), is hypoxia-inducible *in vivo*. This notion is supported by recent studies in cultured cells (Cox et al., 2006). Coexpression of apelin and VEGFA in tumor cells is reminiscent of the angiogenic growth of intersomitic vessels, and thus suggests a similar paracrine function of VEGFA/apelin in tumor angiogenesis.

Clinical significance and therapeutic implications

To date, a limited number of clinical anti-angiogenesis trials utilizing small molecule inhibitors to VEGFA signaling have been performed to treat GBM. However, none of them has yielded a significant clinical benefit (Sun et al., 2006). It appears that tumors evade anti-VEGFA treatment by upregulating additional angiogenic factors. Interestingly, stem cell factor (SCF) was recently discovered as a potent angiogenic factor overexpressed in GBM biopsies (Sun et al., 2006). The consistent upregulation of apelin and APJ expression in GBM reported here introduces now an additional angiogenic signaling pathway. It is therefore likely that apelin, SCF, and VEGFA synergize in promoting angiogenic responses in malignant gliomas and complete inhibition of tumor angiogenesis may require simultaneous disruption of all three signaling pathways. The apelin-APJ signal transduction pathway seems particularly

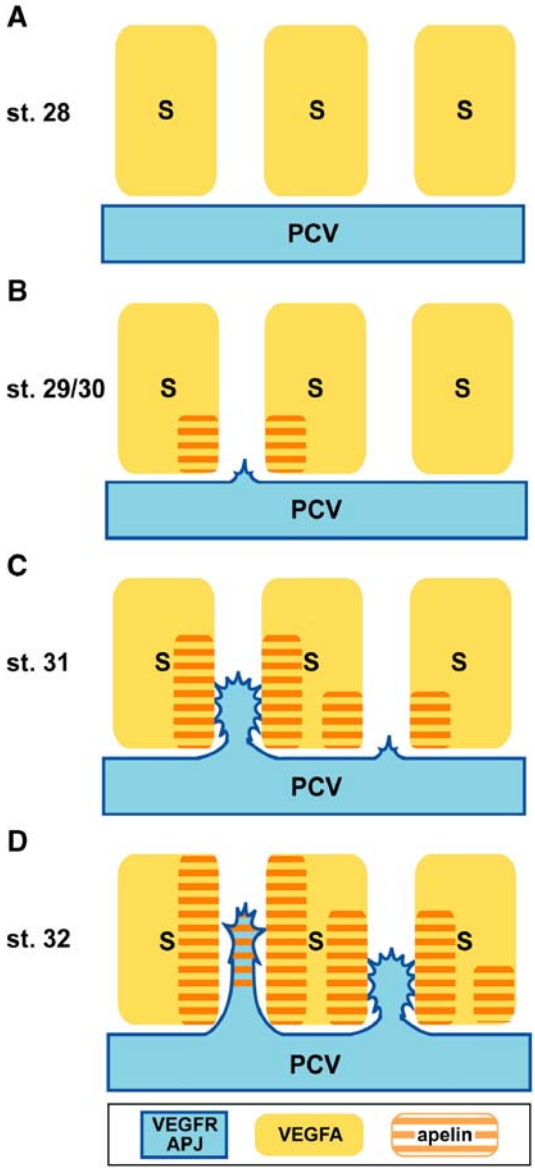

Fig. 6. Model depicting the relationship of apelin and VEGFA signaling during angiogenesis of ISVs in *Xenopus*. The PCV and three somites (S) are shown in lateral view with anterior to the left and dorsal to the top. (A) Prior to the initiation of ISV growth, all somites along the anterioposterior axis express VEGFA. Furthermore, the PCV expresses VEGFRs and APJ and, thus, is competent to respond to VEGFA and apelin, respectively. Paracrine VEGFA signaling primes the PCV for angiogenic sprouting. (B) Apelin expression in dermatomal cell populations flanking the 1st intersomitic space has been initiated and precedes sprouting of the first ISV. (C) Paracrine apelin signaling has triggered sprouting of the ISV. Dermatomal apelin expression spreads dorsally ahead of the ISV growth. Furthermore, apelin expression in the dermatome flanking the 2nd intersomitic space has been initiated. (D) ISV endothelia at the leading edge start to express apelin. Apelin signaling acts now in an autocrine manner to sustain endothelial cell migration. Angiogenic growth of the second ISV is initiated and apelin expression is induced in the dermatome flanking the neighboring, more posterior intersomitic space.

attractive for the development of small-molecule drugs given that APJ encodes a GPCR and thus represents a "drugable" target. In addition, disruption of apelin signaling in *Xenopus* blocks angiogenic blood vessel growth *without* altering preexisting and matured vasculature. Finally, functional screening and preclinical validation of drug candidates can, at least to some extent, be performed in *Xenopus* tadpoles (Brändli, 2004).

Acknowledgments

We thank Atsushi Kitayama and Naoto Ueno for *Xenopus laevis* EST clones; Marianne Petry for excellent technical assistance with *in situ* hybridization analysis on mouse embryos; Silvia Behnke and Bernhard Odermatt for performing *in situ* hybridizations on human tumor samples and Ekkehard Hewer for discussion; and Maya Günthert for technical assistance with confocal microscopy. AWB thanks Adriano Aguzzi for help and advice in initiating the analysis of human tumor samples. This work was supported by grants of the US National Institutes of Health (R01NS046006) to FLH and the Swiss National Science Foundation (3100A0-101964/1) to AWB.

Appendix A. Supplementary data

Supplementary data associated with this article can be found, in the online version, at doi:10.1016/j.ydbio.2007.03.004.

References

Autiero, M., et al., 2003. Role of PlGF in the intra- and intermolecular cross talk between the VEGF receptors Flt1 and Flk1. Nat. Med. 9, 936–943.

Baltzinger, M., et al., 1999. Xl erg: expression pattern and overexpression during development plead for a role in endothelial cell differentiation. Dev. Dyn. 216, 420–433.

Banville, D., Williams, J.G., 1985. The pattern of expression of the *Xenopus laevis* tadpole alpha-globin genes and the amino acid sequence of the three major tadpole alpha-globin polypeptides. Nucleic Acids Res. 13, 5407–5421.

Bertwistle, D., et al., 1996. GATA factors and the origins of adult and embryonic blood in Xenopus: responses to retinoic acid. Mech. Dev. 57, 199–214.

Brändli, A.W., 2004. Prospects for the Xenopus embryo model in therapeutics technologies. Chimia 58, 695–702.

Brändli, A.W., Kirschner, M.W., 1995. Molecular cloning of tyrosine kinases in the early Xenopus embryo: identification of Eck-related genes expressed in cranial neural crest cells of the second (hyoid) arch. Dev. Dyn. 203, 119–140.

Carmeliet, P., 2000. Mechanisms of angiogenesis and arteriogenesis. Nat. Med. 6, 389–395.

Casanovas, O., et al., 2005. Drug resistance by evasion of antiangiogenic targeting of VEGF signaling in late-stage pancreatic islet tumors. Cancer Cell. 8, 299–309.

Cleaver, O., et al., 1997. Neovascularization of the Xenopus embryo. Dev. Dyn. 210, 66–77.

Cory, A.H., et al., 1991. Use of an aqueous soluble tetrazolium/formazan assay for cell growth assays in culture. Cancer Commun. 3, 207–212.

Cox, C.M., et al., 2006. Apelin, the ligand for the endothelial G-protein-coupled receptor, APJ, is a potent angiogenic factor required for normal vascular development of the frog embryo. Dev. Biol. 296, 177–189.

Desideri, G., et al., 2003. Angiotensin II inhibits endothelial cell motility through an AT1-dependent oxidant-sensitive decrement of nitric oxide availability. Arterioscler. Thromb. Vasc. Biol. 23, 1218–1223.

Devic, E., et al., 1996. Expression of a new G protein-coupled receptor X-msr is associated with an endothelial lineage in *Xenopus laevis*. Mech. Dev. 59, 129–140.

Devic, E., et al., 1999. Amino acid sequence and embryonic expression of msr/apj, the mouse homolog of Xenopus X-msr and human APJ. Mech. Dev. 84, 199–203.

Eid, S.R., Brändli, A.W., 2001. Xenopus Na,K-ATPase: primary sequence of the beta2 subunit and in situ localization of alpha1, beta1, and gamma expression during pronephric kidney development. Differentiation 68, 115–125.

Esch, F., et al., 1985. Primary structure of bovine pituitary basic fibroblast growth factor (FGF) and comparison with the amino-terminal sequence of bovine brain acidic FGF. Proc. Natl. Acad. Sci. U. S. A. 82, 6507–6511.

Fan, X., et al., 2003. Structural and functional study of the apelin-13 peptide, an endogenous ligand of the HIV-1 coreceptor APJ. Biochemistry 42, 10163–10168.

Ferrara, N., et al., 2003. The biology of VEGF and its receptors. Nat. Med. 9, 669–676.

Gerhardt, H., et al., 2003. VEGF guides angiogenic sprouting utilizing endothelial tip cell filopodia. J. Cell Biol. 161, 1163–1177.

Goldbrunner, R.H., et al., 2000. Vascular endothelial growth factor-driven glioma growth and vascularization in an orthotopic rat model monitored by magnetic resonance imaging. Neurosurgery 47, 921–929 discussion 929-30.

Goldbrunner, R.H., et al., 2004. PTK787/ZK222584, an inhibitor of vascular endothelial growth factor receptor tyrosine kinases, decreases glioma growth and vascularization. Neurosurgery 55, 426–432 (discussion 432).

Habata, Y., et al., 1999. Apelin, the natural ligand of the orphan receptor APJ is abundantly secreted in the colostrum. Biochim. Biophys. Acta 1452, 25–35.

Hashimoto, Y., et al., 2005. G protein-coupled APJ receptor signaling induces focal adhesion formation and cell motility. Int. J. Mol. Med. 16, 787–792.

Hatva, E., et al., 1995. Expression of endothelial cell-specific receptor tyrosine kinases and growth factors in human brain tumors. Am. J. Pathol. 146, 368–378.

Helbling, P.M., et al., 1998. Requirement for EphA receptor signaling in the segregation of Xenopus third and fourth arch neural crest cells. Mech. Dev. 78, 63–79.

Helbling, P.M., et al., 1999. Comparative analysis of embryonic gene expression defines potential interaction sites for Xenopus EphB4 receptors with ephrin-B ligands. Dev. Dyn. 216, 361–373.

Helbling, P.M., et al., 2000. The receptor tyrosine kinase EphB4 and ephrin-B ligands restrict angiogenic growth of embryonic veins in *Xenopus laevis*. Development 127, 269–278.

Hermanson, M., et al., 1992. Platelet-derived growth factor and its receptors in human glioma tissue: expression of messenger RNA and protein suggests the presence of autocrine and paracrine loops. Cancer Res. 52, 3213–3219.

Holland, E.C., 2001. Gliomagenesis: genetic alterations and mouse models. Nat. Rev., Genet. 2, 120–129.

Hosoya, M., 2000. Molecular and functional characteristics of, A.P.J. tissue distribution of mRNA and interaction with the endogenous ligand apelin. J. Biol. Chem. 275, 21061–21067.

Inui, M., et al., 2006. Xapelin and Xmsr are required for cardiovascular development in *Xenopus laevis*. Dev. Biol. 298, 188–200.

Iraha, F., et al., 2002. Common and distinct signals specify the distribution of blood and vascular cell lineages in *Xenopus laevis* embryos. Dev. Growth Differ. 44, 395–407.

Ishida, J., et al., 2004. Regulatory roles for APJ a seven-transmembrane receptor related to angiotensin-type 1 receptor in blood pressure in vivo. J. Biol. Chem. 279, 26274–26279.

Kasai, A., et al., 2004. Apelin is a novel angiogenic factor in retinal endothelial cells. Biochem. Biophys. Res. Commun. 325, 395–400.

Keck, P.J., et al., 1989. Vascular permeability factor, an endothelial cell mitogen related to PDGF. Science 246, 1309–1312.

Kerbel, R.S., 2006. Antiangiogenic therapy: a universal chemosensitization strategy for cancer? Science 312, 1171–1175.

Kleihues, P., et al., 2002. The WHO classification of tumors of the nervous system. J. Neuropathol. Exp. Neurol. 61, 215–225 (Discussion 226-9).

Kleinz, M.J., Davenport, A.P., 2005. Emerging roles of apelin in biology and medicine. Pharmacol. Ther. 107, 198–211.

Kleinz, M.J., et al., 2005. Immunocytochemical localisation of the apelin receptor, APJ, to human cardiomyocytes, vascular smooth muscle and endothelial cells. Regul. Pept. 126, 233–240.

Korff, T., Augustin, H.G., 1998. Integration of endothelial cells in multicellular spheroids prevents apoptosis and induces differentiation. J. Cell Biol. 143, 1341–1352.

Korff, T., Augustin, H.G., 1999. Tensional forces in fibrillar extracellular matrices control directional capillary sprouting. J. Cell Sci. 112 (Pt. 19), 3249–3258.

Lee, D.K., et al., 2005. Modification of the terminal residue of apelin-13 antagonizes its hypotensive action. Endocrinology 146, 231–236.

Leung, D.W., et al., 1989. Vascular endothelial growth factor is a secreted angiogenic mitogen. Science 246, 1306–1309.

Masri, B., et al., 2004. Apelin (65–77) activates p70 S6 kinase and is mitogenic for umbilical endothelial cells. FASEB J.

Masri, B., et al., 2005. Apelin signalling: a promising pathway from cloning to pharmacology. Cell Signal. 17, 415–426.

Medhurst, A.D., et al., 2003. Pharmacological and immunohistochemical characterization of the APJ receptor and its endogenous ligand apelin. J. Neurochem. 84, 1162–1172.

Meyer, D., et al., 1995. Whole-mount in situ hybridization reveals the expression of the Xl-Fli gene in several lineages of migrating cells in Xenopus embryos. Int. J. Dev. Biol. 39, 909–919.

Millard, N., 1949. The development of the venous system of *Xenopus laevis*. Trans. R. Soc. S. Afr. 32, 55–99.

Mizukami, Y., et al., 2005. Induction of interleukin-8 preserves the angiogenic response in HIF-1alpha-deficient colon cancer cells. Nat. Med. 11, 992–997.

Moody, S.A., Kline, M.J., 1990. Segregation of fate during cleavage of frog (*Xenopus laevis*) blastomeres. Anat. Embryol. 182, 347–362.

Nitta, H., et al., 2003. Application of automated mRNA in situ hybridization for formalin-fixed, paraffin-embedded mouse skin sections: effects of heat and enzyme pretreatment on mRNA signal detection. Appl. Immunohistochem. Mol. Morphol. 11, 183–187.

O'Dowd, B.F., et al., 1993. A human gene that shows identity with the gene encoding the angiotensin receptor is located on chromosome 11. Gene 136, 355–360.

Plate, K.H., Risau, W., 1995. Angiogenesis in malignant gliomas. Glia 15, 339–347.

Plate, K.H., et al., 1992. Vascular endothelial growth factor is a potential tumour angiogenesis factor in human gliomas in vivo. Nature 359, 845–848.

Poole, T.J., Coffin, J.D., 1989. Vasculogenesis and angiogenesis: two distinct morphogenetic mechanisms establish embryonic vascular pattern. J. Exp. Zool. 251, 224–231.

Reaux, A., et al., 2001. Physiological role of a novel neuropeptide, apelin, and its receptor in the rat brain. J. Neurochem. 77, 1085–1096.

Saint-Geniez, M., et al., 2002. Expression of the murine msr/apj receptor and its ligand apelin is upregulated during formation of the retinal vessels. Mech. Dev. 110, 183–186.

Saitou, N., Nei, M., 1987. The neighbor joining method: a new method for reconstructing phylogenetic trees. Mol. Biol. Evol. 4, 406–425.

Saulnier, D.M., 2002. Essential function of Wnt-4 for tubulogenesis in the Xenopus pronephric kidney. Dev. Biol. 248, 13–28.

Stupp, R., et al., 2005. Optimal role of temozolomide in the treatment of malignant gliomas. Curr. Neurol. Neurosci. Rep. 5, 198–206.

Sun, L., et al., 2006. Neuronal and glioma-derived stem cell factor induces angiogenesis within the brain. Cancer Cell 9, 287–300.

Tatemoto, K., et al., 1998. Isolation and characterization of a novel endogenous peptide ligand for the human APJ receptor. Biochem. Biophys. Res. Commun. 251, 471–476.

Turner, D.L., Weintraub, H., 1994. Expression of achaete-scute homolog 3 in Xenopus embryos converts ectodermal cells to a neural fate. Genes Dev. 8, 1434–1447.

Wilkinson, D.G., 1992. Whole mount in situ hybridization of vertebrate embryos. In: Wilkinson, D.G. (Ed.), In situ Hybridization: A Practical Approach. Oxford University Press, Oxford, pp. 75–84.

Yao, Y., et al., 2001. Prognostic value of vascular endothelial growth factor and its receptors Flt-1 and Flk-1 in astrocytic tumours. Acta Neurochir. (Wien) 143, 159–166.

Zhou, N., et al., 2003. Cell-cell fusion and internalization of the CNS-based, HIV-1 co-receptor, APJ. Virology 307, 22–36.